Synthesis and Characterization of Carboxylate Complexes of Sn^{IV} Porphyrin Monomers and Oligomers

Joanne C. Hawley, Nick Bampos,* and Jeremy K. M. Sanders[a]

Abstract: Most of the porphyrin-recognition chemistry we have investigated previously has centred on kinetically labile metal–ligand interactions, such as Zn–N and Ru–N. Our interest in the broader scope of molecular recognition required a metal with the ability to specifically recognise non-nitrogen-based ligands, with a significantly different binding interaction to distinguish it from nitrogen-based analogues. In this report we describe interactions of Sn^{IV} porphyrins that bind oxygen-based ligands and for which the Sn^{IV}–O bond is in slow exchange on the NMR timescale. A series of carboxylate complexes is employed to highlight the structural/geometric features of porphyrin monomers and cyclic oligomers. Where more than one porphyrin unit is present in a molecular scaffold, we report the effect of carboxylate binding on the complex when the two porphyrins contain different metals (typically Sn^{IV} and Zn^{II}). The unexpected spectroscopic and structural properties of the Sn_2(9-anthroic acid)-porphyrin dimer are also reported.

Keywords: carboxylate ligands · molecular recognition · O ligands · porphyrinoids · tin · zinc

Introduction

As part of a larger project aimed at supramolecular catalysis[1, 2] we have been exploring the ligand-recognition properties of tin(IV) porphyrins. Here we outline the synthesis and solution-state geometry of tin(IV) porphyrin carboxylate complexes and detail how anthracene–porphyrin interactions can overcome the usual geometrical preferences.[3]

The formation of a Sn^{IV} porphyrin carboxylate complex from a carboxylic acid and Sn^{IV} dihydroxo porphyrin in the absence of an external reagent and with the elimination of water as a side product, was viewed as a potentially useful recognition event for supramolecular chemistry. With this in mind, $Sn(OH)_2$ porphyrins and $Sn(OH)_2$ analogues of porphyrin oligomers, previously described by our group,[4] were prepared in order to explore the Sn porphyrin–carboxylate binding interaction and recognition properties of $Sn(OH)_2$ porphyrin oligomers (**2**–**4**). In particular, $Sn(OH)_2$Zn-2,2-dimer **3** was designed to incorporate Sn and Zn porphyrins and thereby extend this study to the simultaneous binding of N and O ligands.[5]

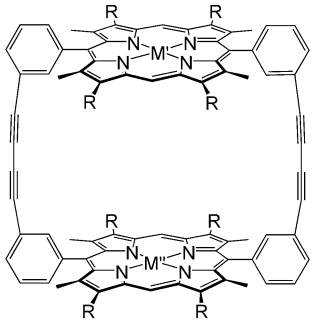

M'	M''	
$SnCl_2$	$SnCl_2$	**1**
$Sn(OH)_2$	$Sn(OH)_2$	**2**
$Sn(OH)_2$	Zn	**3**

R = $CH_2CH_2CO_2CH_3$

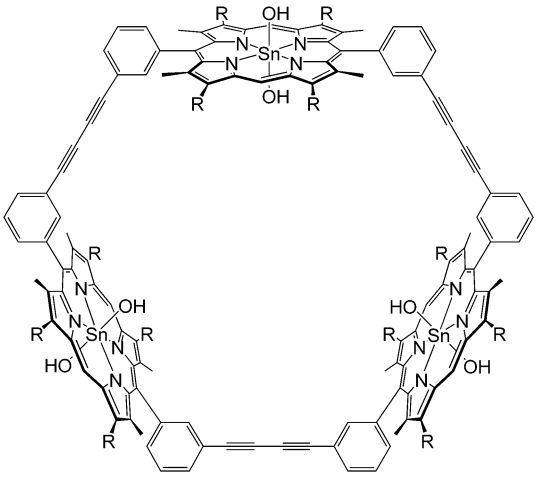

4

R = $CH_2CH_2CO_2CH_3$

In this report we detail the syntheses of $SnCl_2$ and $Sn(OH)_2$ porphyrins, the development of methodology for the synthesis of $Sn(OH)_2$ porphyrin oligomers and different methods by which dicarboxylate complexes may be prepared. The spectroscopic properties of Sn porphyrins and their carboxylate

[a] Dr. N. Bampos, Dr. J. C. Hawley, Prof. J. K. M. Sanders
University Chemical Laboratory, University of Cambridge
Lensfield Road, Cambridge, CB2 1EW (UK)
E-mail: nb10013@cam.ac.uk

 DOI: 10.1002/chem.200304862

analogues are discussed, with an emphasis on the geometry of Sn porphyrin carboxylate complexes, as determined from NOE experiments and ring current modelling. Some of the results have been summarised elsewhere,[6] but we have subsequently built on the results described here to create larger assemblies using Sn carboxylate complexes.[7]

Results and Discussion

Preparation of Sn porphyrin monomers: Typically Sn is inserted into porphyrins by using Sn dichloride dihydrate ($SnCl_2 \cdot 2H_2O$ in the presence of pyridine) to give the $SnCl_2$ complex of the porphyrin, which is then hydrolysed quantitatively in situ (aqueous ammonia in the presence of pyridine) to the corresponding $Sn(OH)_2$ porphyrin.[8, 9] Since the work described here was carried out, an alternative method for inserting Sn into porphyrins has been published.[10]

The reaction time required for the complete metallation of the free-base porphyrin monomer **5**[4] under literature conditions to form **6** varied considerably, and for this reason an assay for Sn insertion was developed. As residual pyridine affected the elution of porphyrins on thin-layer chromatography (tlc), UV spectroscopy was preferred as a means of following Sn insertion.[11] A drop of the reaction mixture was diluted with chloroform, and the disappearance of the lowest-wavelength Q-band, diagnostic of metallation, was monitored.

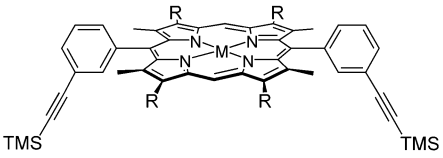

M = H_2 **5**
M = $SnCl_2$ **6**
M = $Sn(OH)_2$ **7**

R = $CH_2CH_2CO_2CH_3$

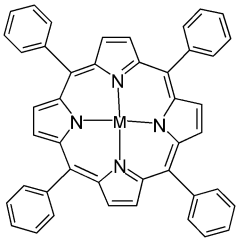

M = H_2 **8**
M = $SnCl_2$ **9**
M = $Sn(OH)_2$ **10**

The standard method of hydrolysis of $SnCl_2$ porphyrins proved unsuitable for the transformation of $SnCl_2$ monomer **6** to $Sn(OH)_2$ monomer **7** as, in the presence of ammonia, the peripheral ester groups would be susceptible to hydrolysis.[7] Typically, a milder technique employing basic deactivated alumina, which had previously been reported, was adopted.[12] A solution of $SnCl_2$ porphyrin was stirred with alumina and subsequently filtered or passed through a short column of alumina. In the presence of alumina, ethanol and $Sn(OH)_2$, porphyrins form $SnCl_2$ porphyrin ethoxide complexes; high-field ^{1}H NMR resonances with characteristic ethyl multiplets in addition to *meso*- and β-pyrrole signals indicate tin-bound ethoxide. To prevent contamination by alcohols, which tend to coordinate to the Sn site, all chloroform was filtered through basic alumina (activity V) prior to use. In this way $Sn(OH)_2$ monomer **7** was prepared cleanly and in good yield, typically 80% from the free-base porphyrin or 90% from the dichloroporphyrin. Tetraphenylporphyrines $SnCl_2$TPP (**9**) and $Sn(OH)_2$TPP (**10**) were similarly prepared by the method described above. Sn insertion into H_2TPP **8** proceeded more readily than for H_2 monomer **5**, and it was generally not necessary to employ a large excess of Sn dichloride or long reaction times. Conversion of **9** to **10** in the presence of alumina, however, required extended periods of stirring; this may reflect the importance of the solubility of the porphyrin under investigation. In the preparations we report here, activated and neutral alumina were found to be far less efficient than basic activity V alumina in effecting the reaction. Stirring $SnCl_2$ porphyrins with water under parallel conditions in the absence of alumina did not result in the formation of Sn−OH groups.

To monitor the hydrolysis of $SnCl_2$ porphyrins, an aliquot of the reaction mixture was removed and analysed by ^{1}H NMR spectroscopy; small shifts in the resonances of the propionate and pyrrole methyl protons of **6**, and an upfield displacement of the *meso* resonance (or β-pyrrole resonance of TPP) were indicative of hydrolysis. In mixtures of $SnCl_2$, SnCl(OH) and $Sn(OH)_2$ porphyrins, the *meso* (or β-pyrrole) resonances attributable to the three porphyrin species were resolved in a very confined region of the spectrum ($\sim$9.2 ppm for the β-pyrrole or $\sim$10.1 ppm for the *meso* protons), while the Sn−OH resonance of $Sn(OH)_2$ porphyrins in [D]chloroform were broad and not diagnostic of the progress of the reaction. In the UV/Vis spectrum, a shift of $\sim$1 nm is typically observed in the Soret band characterising the conversion of $SnCl_2$ to $Sn(OH)_2$ porphyrins; this could not be conveniently, or reliably, used to follow the reaction.

Sn porphyrin dicarboxylate complexes, such as **11**–**14** (the porphyrin macrocycle has been represented as bar, as if viewed from the side, for clarity), have traditionally been prepared by stirring a $Sn(OH)_2$ porphyrin with an excess of a carboxylic acid and recrystallising the product from the unreacted acid.[13] However, this is clearly unsuitable for acids which are themselves solid. In our work, Sn porphyrin dicarboxylate complexes, such as **15**–**17**, for which diagnostic ^{1}H NMR chemical shifts of the bound ligand are shown in Figure 1, were generally prepared on a small scale in the presence of just two equivalents of carboxylic acid. For the accurate addition of stoichiometric quantities, a stock solution of the carboxylic acid was prepared in [D]chloroform or a mixture of [D]chloroform and [D_4]methanol, depending

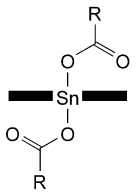

RCO_2H
$CH_3CH_2CO_2H$ **11**
CH_3CO_2H **12**
$ClCH_2CO_2H$ **13**
Cl_2CHCO_2H **14**

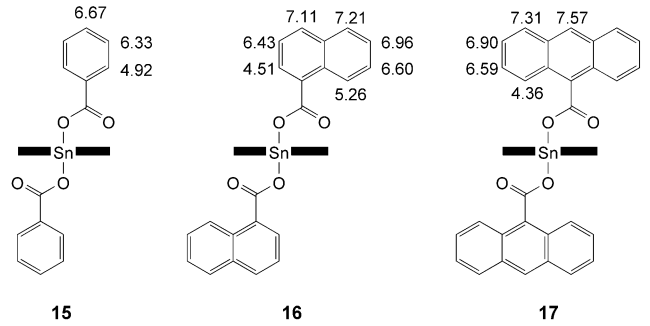

Figure 1. The structures of Sn porphyrin complexes **15**, **16** and **17**, obtained by the addition of benzoic, 1-naphthoic or 9-anthroic acid, respectively, to $Sn(OH)_2$ porphyrin **10**. ^{1}H NMR chemical shifts (ppm) are shown for selected ligand sites (proton atoms have been omitted for clarity) to indicate the effect of the ring current as a function of distance from the porphyrin plane. $\Delta\delta$ values were difficult to calculate as the organic acids were sparingly soluble in chloroform, with resonances congested in a small range near the residual solvent resonance.

on the solubility of the carboxylic acid. Acids which were insoluble in [D]chloroform at mM concentrations could be added as a solid to a stirred solution of $Sn(OH)_2$ porphyrin to give the corresponding dicarboxylate complex (for example **18** and **19**). If nonstoichiometric quantities of polar acids were employed, the difficulty of removing excess acid arose; Sn porphyrin dicarboxylate complexes do not survive chromatography on alumina. Compounds **18** and **19** provide examples of the diverse structures that may be created with Sn porphyrins and carboxylates, and illustrate the potential for constructing larger, more complex supramolecular systems. In both cases, despite the complex nature of the structures and the congestion encountered in the ^{1}H NMR spectrum, the structures were identified by the diagnostic change in the chemical shifts of specific ligand and porphyrin resonances as a result of the distance-dependent porphyrin ring current (Figure 2). A mechanism for the addition of the carboxylic acid has been proposed by us previously,[3] and has subsequently been applied to the addition of alcohols to Sn-porphyrins.[14]

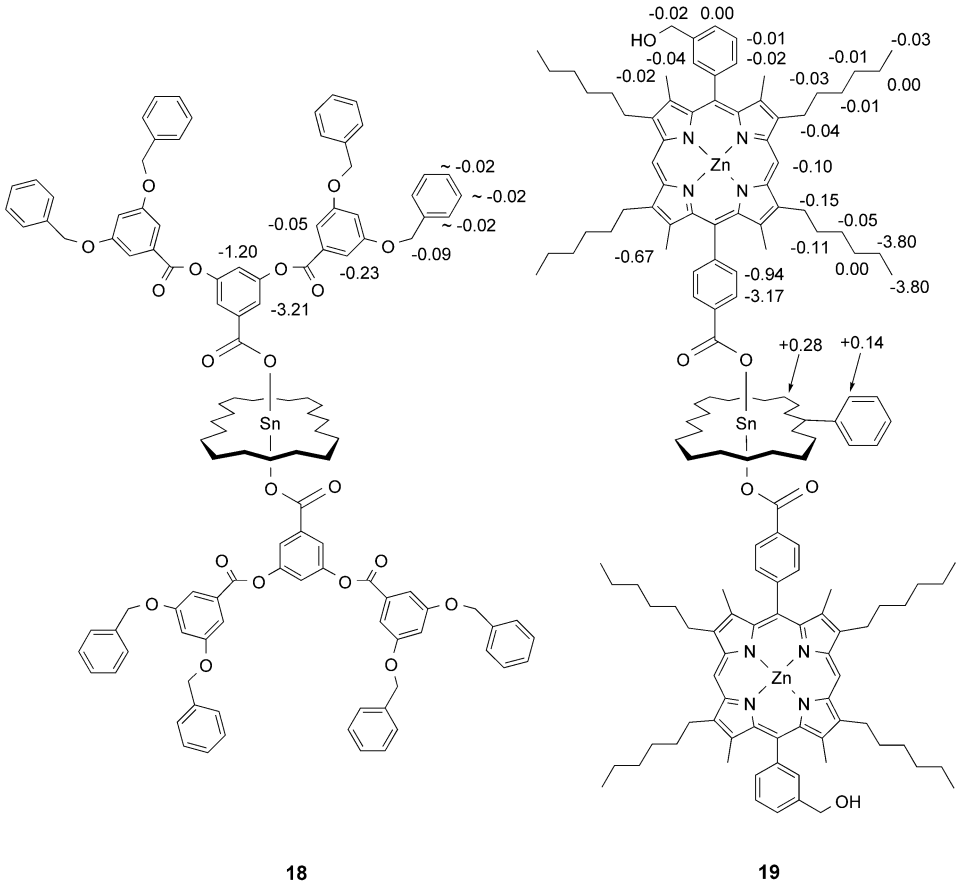

Figure 2. Compounds **18** and **19** offer examples of the type of nontrivial structures that can be generated by using the methodology outlined in the text. $\Delta\delta$ values are presented to conveniently map the selected proton chemical shifts (ppm) as a function of their position relative to the neighbouring ring currents. (The proton atoms and peripheral substituents of the Sn porphyrin lacking diagnostic significance have been omitted from the structures for clarity.)

As carboxylate ligands are in slow exchange with Sn porphyrins on the NMR timescale, their protons always give sharp, well-defined resonances at room temperature.[3] Furthermore, as a consequence of experiencing the porphyrin ring current, carboxylate-ligand protons resonate at high field, usually clear of the porphyrin resonances—for example, the acetate protons of $Sn(acetate)_2TPP$, **12**, resonate at $\delta_H = -1.0$ ppm. The magnitude of the upfield shift that a carboxylic acid proton experiences on formation of a Sn porphyrin carboxylate complex is dependent on the distance of the proton from the porphyrin plane. This can be seen by the methylene resonances of propionic acid in $Sn(propionate)_2TPP$, **11**, which sit closer to the porphyrin plane and are consequently displaced upfield by 0.6 ppm more than the methyl resonances. However, the difference in the chemical shifts of free carboxylic acid protons and the corresponding Sn porphyrin carboxylate protons may also reflect the electronic change that takes place (going from a carboxylic acid to a carboxylate anion).

Substitution of the hydroxo ligands of a Sn porphyrin by a carboxylate group caused a blue shift of the porphyrin Soret band, but one which was too small (1 – 2 nm) to allow ligand exchange to be conveniently monitored by UV spectroscopy. For a selection of dicarboxylate complexes of SnTPP derived from aliphatic carboxylic acids, the Soret band appeared within a range of 1 – 2 nm about 420 nm and was therefore not

particularly diagnostic. Attempts to characterise dicarboxylate complexes of Sn porphyrins and dihydroxo Sn porphyrins by mass spectrometry were unsuccessful; in FIB and FAB mass spectrometry, the Sn porphyrin axial ligands were displaced and an adduct of the matrix was observed. Using MALDI-TOF mass spectrometry without a suitable matrix proved difficult as once again ligand loss was detected, while reproducibility of spectra was problematic.

Preparation of Sn porphyrin oligomers: Essentially the same methods were employed for the preparation of Sn complexes of cyclic oligomers of **5** as were used for **6** and **7**, described above. Sn insertion into the H_4-2,2 dimer **20** was achieved with minor optimisation; larger volumes of pyridine were used to prevent the precipitation of porphyrinic material. After isolation on Celite, the crude product could not be redissolved in chloroform. Most of the pyridine present was removed by distillation under reduced pressure, and the residual concentrated solution was then diluted with chloroform and cautiously washed with hydrochloric acid and water.

Stirring dimer **1** with alumina in chloroform resulted in significant problems with the solubility and isolation. An alternative stationary phase was sought to promote the hydrolysis of $SnCl_2$ porphyrin oligomers. The most promising results were obtained with diaion resin WA30 (Supelco), a weak anion-exchange resin having basic functionality. The addition of water to a slurry of the resin and $SnCl_2$ porphyrin in chloroform improved the efficiency of the hydrolysis, paralleling the better results obtained with deactivated alumina relative to dry alumina. By using 100 molar equivalents of resin to porphyrin and 1000 molar equivalents of water, complete hydrolysis of $SnCl_2$ porphyrin oligomers was typically achieved in four hours, as determined by ^{1}H NMR spectroscopy. Small shifts in the resonances of the oligomers allowed the extent of reaction to be monitored, similarly to the hydrolysis of $SnCl_2$ monomers. The formation of Sn–OH groups was confirmed by adding acetic acid to a sample of the reaction mixture and observing the formation of the bound acetate groups by ^{1}H NMR spectroscopy.[15] Acetic acid was selected for this purpose due to the rapid binding of the acetate groups to $Sn(OH)_2$ porphyrins and the single characteristic (methyl) high-field resonance detected in the ^{1}H NMR spectrum. Adopting the diaion-resin-hydrolysis methodology enabled dimer **2** and 2,2,2-trimer **4** to be prepared, but the latter was severely hindered by poor solubility.

In order to prepare the mixed metalloporphyrin dimer **3**, a different approach was required. A templated Glaser–Hay coupling of alkyne-functionalised $Sn(OH)_2$ and Zn porphyrins to give **3** was not expected to be feasible; removal of a pyridylcarboxylate template would demetallate the Zn porphyrin and necessitate the reinsertion of Zn, with potential contamination of the Sn porphyrin component. Furthermore, the limited scope for purification of the desired compound from the polymeric material typically produced by Glaser–Hay couplings was anticipated to be prohibitively difficult.

A stepwise route to the $Sn(OH)_2$Zn dimer was therefore favoured. The reaction scheme illustrated (Scheme 1) was designed to exploit the variation in the chromatographic mobilities of differentially metallated porphyrins, and to involve Sn insertion as late as possible in the synthesis. To achieve asymmetry, a substoichiometric quantity of Zn was inserted into H_4 dimer **20** to give a statistical mixture of **20**, **21** and **22**. Dimer **20** was separated relatively easily from H_2Zn dimer **21** and Zn_2 dimer **22** by using neutral alumina to provide a monometallated dimer (**21**) into which Sn could be inserted, thereby avoiding the difficult separation of **21** and **22** at this point in the reaction scheme. Partial Zn metallation and chromatography were typically carried out on 200 mg of

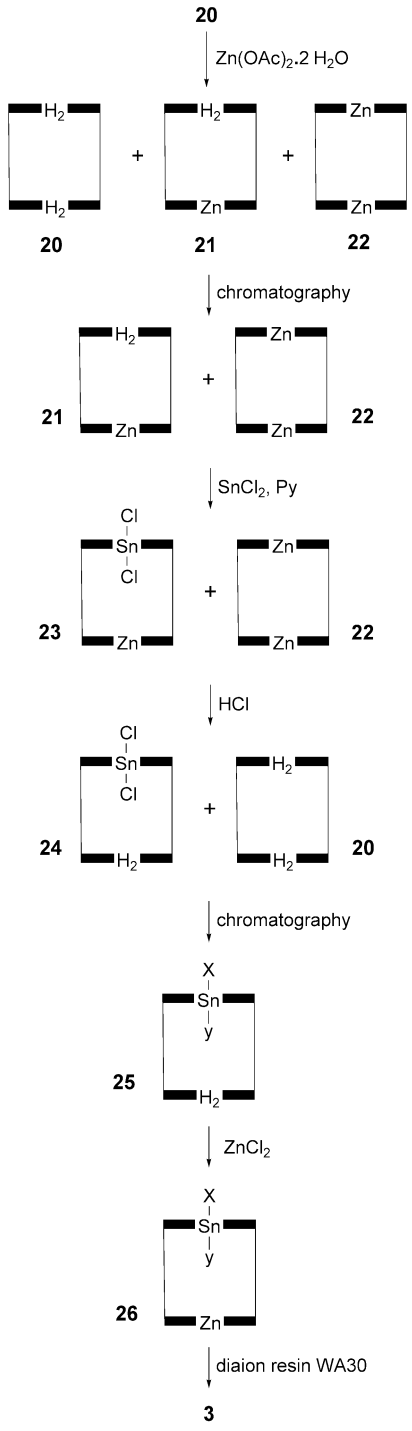

Scheme 1. The reaction and separation sequence for the preparation of the Sn,Zn dimer **3** from the metal-free dimer **20**.

H_4-2,2 dimer. Alumina tlc and ^{1}H NMR were employed to identify the various fractions.

The reaction of anhydrous Sn dichloride with **21** in the presence of dimer **22** proceeded without transmetallation of the Zn porphyrins or solubility difficulties. To facilitate the separation of the two remaining compounds by alumina, however, it was important to increase the chromatographic separation of the constituents, to tolerate any hydrolysis of the Sn porphyrins and to minimise any demetallation of the zinc porphyrin components during separation that might lead to inseparable mixtures of (more than two) compounds. These requirements were best achieved by removal of zinc from the **23**/**22** mixture to allow the easy separation by preparative alumina tlc of the mono Sn dimer from H_4 dimer **20**. Chromatography of the Sn-substituted dimer **24** on alumina resulted in hydrolysis of some Sn-chloro groups producing $SnCl_X(OH)_YH_2$-2,2 dimer ($X + Y = 2$) **25**. The ^{1}H NMR spectrum of **25** exhibited two broad NH pyrrole resonances in the high-field region that were attributed to dimers in which there was a hydroxo group on the inner Sn porphyrin face and dimers in which there was a chloro group at the inner site.

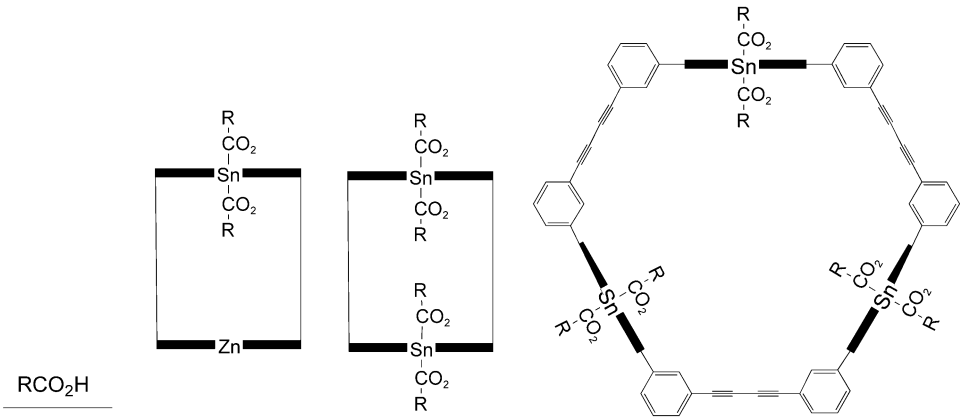

RCO_2H			
	**27**	**31**	**35**
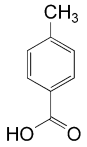	**28**	**32**	**36**
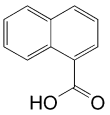	**29**	**33**	
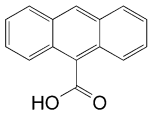	**30**	**34**	

Zn insertion into dimer **25** was carried out with zinc dichloride, rather than zinc acetate, to prevent the complexation of acetate groups at Sn–OH sites. The hydrolysis of $SnCl_X(OH)_YZn$-2,2 dimer **26**, thus obtained, was completed by stirring it with diaion resin, thereby providing **3** in 16% overall yield from **20** (300 mg of **20**). Retention of porphyrin on alumina was believed to be the major source of lost product.

Aliquots of a range of carboxylic acids were added to $Sn(OH)_2$ porphyrin oligomers; this allowed preparation of a variety of carboxylate complexes of Sn porphyrin dimers and trimers (**27** – **36**). In each case, the proton resonances in the ^{1}H NMR spectrum attributed to the added acid disappeared, and multiple ligand resonances were observed; this is consistent with coordination to both the inner and outer Sn porphyrin faces. Comparison of the ligand chemical shifts of carboxylate complexes of cyclic Sn porphyrin oligomers to those of a monomeric complex of the same carboxylate provided some indication of which resonances were attributable to the inner ligand and which to the outer ligand, yet the unambiguous assignment necessitated 2D NMR experiments.

Effect of binding on the host geometry: In the absence of crystal structures of monomeric Sn porphyrin complexes, ^{1}H NMR properties were used to identify the features that reveal the complexes' geometry. The large carboxylate-resonance shift that occurs when carboxylate groups bind to Sn porphyrins, and the fact that the resulting complexes are in slow exchange, render Sn porphyrin carboxylate complexes suitable for a computational analysis that calculates the shift ($\Delta\delta$) of ligand ^{1}H NMR resonances on binding to porphyrins.[16] In the model we applied, the porphyrin ring current was parameterised for a particular class of metalloporphyrin, and all the atoms of the complex were defined in three-dimensional space. These "input" atom coordinates, particularly of the bound ligand, may be changed by some incremental value in order to search various ligand bond lengths, angles and dihedral angles. Several such parameters may be floated, either individually or in combination and, in this way, $\Delta\delta$ may be generated for different geometries and compared against $\Delta\delta_{obs}$ to determine which exhibits the best agreement.

The experimental and predicted chemical shifts for Sn(9-anthroate)$_2$TPP, **17**, were consistent only with a geometry in which the aromatic plane of the ligand was almost parallel to the plane of the porphyrin—more precisely in which the Sn-O-C-C dihedral angle (ϕ) was $\sim 100^\circ$. In the solid state, the aromatic plane of the ligand of Sn(benzoate)$_2$TPP **15** is almost perpendicular to the plane of the porphyrin,[17] while the solution-state structure, based on the NMR-data modelling,

indicated that the dihedral ϕ did not significantly deviate from 180°. The Sn-O-C-C dihedral angle of Sn(1-naphthoate)$_2$TPP, **16**, corresponding to the best agreement between $\Delta\delta_{obs}$ and $\Delta\delta_{calcd}$, was between that for the analogous benzoate and 9-anthroate complexes. The angle between the aromatic planes of these ligands and porphyrin were determined to be smallest in **17** and progressively larger in **16**, and then **15**. If the carbonyl group of 9-anthroate in **17** is orthogonal to the aromatic plane, as in 9-anthroic carboxylic acid,[18] and orientated towards the plane of the porphyrin, as in the crystal structures of other dicarboxylate complexes of Sn porphyrins, then molecular model building shows that the aromatic planes of the ligand and porphyrin will be nearly coplanar.

It is proposed that an attractive $\pi-\pi$ or donor–acceptor interaction between the aromatic components of the ligand and porphyrin of **17** account for their coplanar conformation. If a $\pi-\pi$ interaction brought the 9-anthroate group into proximity of the porphyrin plane, the intermediate spatial requirements of the 1-naphthoate ligand of Sn(1-naphthoate)$_2$TPP between its benzoate and 9-anthroate analogues may be correlated with respect to the size of their π-electron systems.

The slowly exchanging Sn porphyrin-carboxylate binding interaction and the large *trans* cavity ring current of cyclic porphyrin oligomers facilitated the ^{1}H NMR characterisation of carboxylate complexes of **2**, **3** and **4**. The ^{1}H NMR spectrum of each example was assigned with the aid of COSY and NOESY experiments. For example, formation of a single carboxylate complex on addition of two equivalents of 1-naphthoic acid to dimer **3** was evident from the observation of a single (new) set of porphyrin resonances in the ^{1}H NMR spectrum. In sharp contrast, the resulting COSY spectrum of **29** established separate spin systems for the inner and outer ligands, while NOE cross-peaks between protons of the separate ligand spin systems to the porphyrin on which they are both bound made the assignment of the ligand resonances possible. Significantly, NOE connectivities were observed between one of the two ligands and both porphyrins of the "host" dimer, thereby providing definitive evidence for intracavity coordination and identifying the inner bound ligand (Figure 3). The porphyrin resonances of **29** could be assigned on the assumption that the *meso* protons of the Sn and Zn moieties resonated with the same relative chemical shifts as the *meso* protons of the constituent Sn and Zn monomers, and then following the NOE cross-peaks and *J* coupling around the porphyrin. Alternatively, to unambiguously assign the porphyrin resonances, the connectivity from the Sn and Zn porphyrin inner *o-aryl* protons could be followed (Figure 3).

With the exception of the Sn$_2$(9-anthroate)$_4$-2,2 dimer **34** (see below), the ^{1}H NMR spectra of tetracarboxylate complexes of Sn$_2$ dimers and hexacarboxylate complexes of Sn$_3$ trimers were assigned in the same way as described for the Sn(1-naphthoate)$_2$Zn-2,2 dimer **29**. However, carboxylate complexes of **2** and **4**, in which the constituent porphyrins were equivalent, with the overall molecule exhibiting a high degree of symmetry, it was not possible to specify to which porphyrin a particular ligand proton exhibited a host–guest

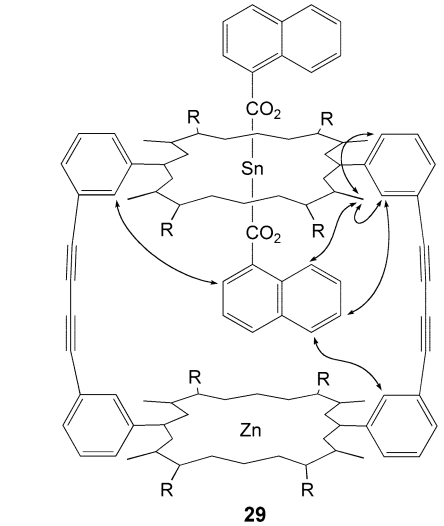

29

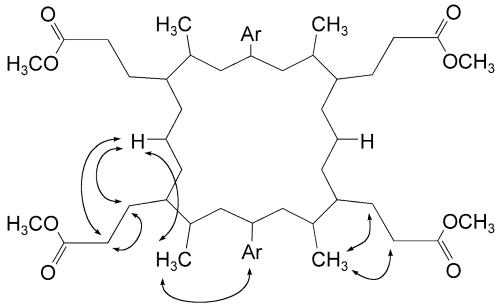

Figure 3. Diagnostic NOE connectivities (^{1}H NOESY) used to characterise intracavity binding are shown as arrows between proton-bearing sites. (The proton atoms have been omitted for clarity.) Compound **29** was chosen as an example, as the second porphyrin contains a zinc atom that ensures that the 1-naphthoic acid inside the cavity is only bound to the Sn porphyrin. Comparable extracavity NOE connectivities are detected between the Sn porphyrin and the extracavity ligand, but not shown here. Through-space (NOE) connectivities are observed across the porphyrin plane as shown by the arrows around the periphery of a representative porphyrin molecule, above (lower representation). Such connectivities (in addition to *J* coupling determined from COSY experiments) are important in identifying the resonances of a particular porphyrin in a cyclic oligomer from the congestion that characterises the ^{1}H NMR spectra.

NOE interaction, although in most cases this could be inferred.

The observation of host–guest NOEs in carboxylate complexes of Sn porphyrin oligomers provided the most effective and reliable means of assigning their spectra (Figure 4). For example, the absence of some diagnostic NOEs between Sn(RCO$_2$)$_2$Zn-2,2 and Sn$_2$(RCO$_2$)$_4$-2,2 dimer porphyrin protons and ligands bound to the outer face implied that the coordinated Sn porphyrin might be domed so that the Sn ion was displaced away from the centre of the cavity, with the bound ligands (outer face) consequently further from the porphyrin plane. By contrast, the observation of NOE correlations between the porphyrin *o-aryl* protons and both the inner and outer ligands of Sn$_3$(*p*-toluate)$_6$-2,2,2 trimer **36** indicated that the constituent porphyrins were less distorted than in the analogous dimer complexes. An important insight into the geometry and flexibility of porphyrin oligomers based

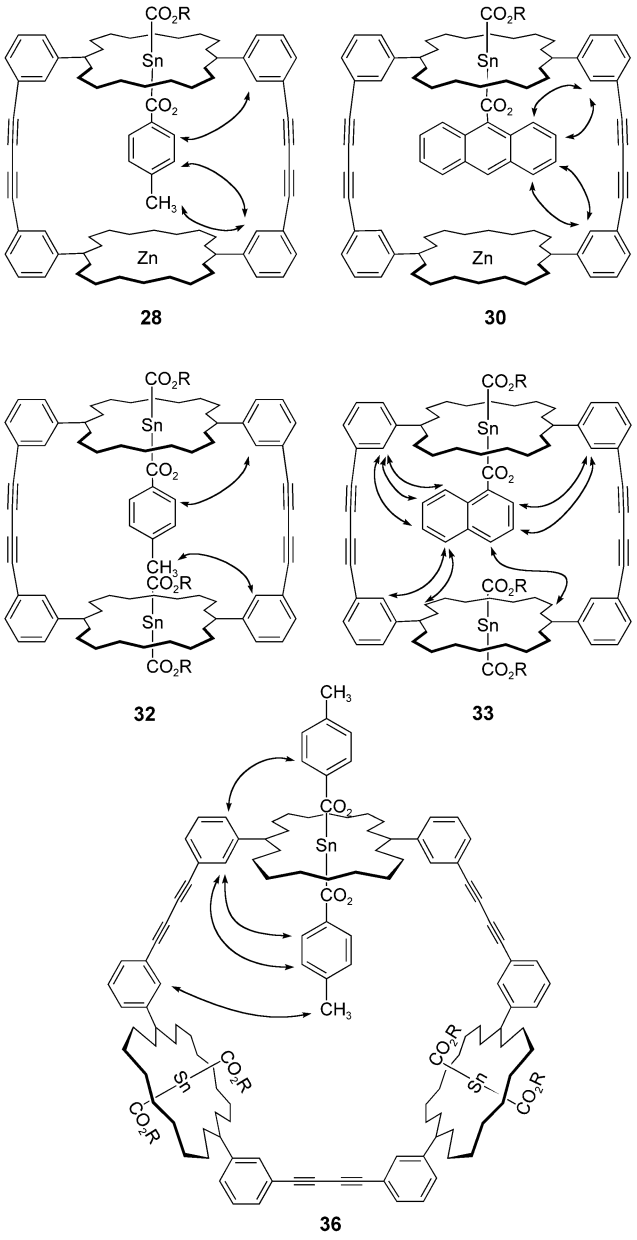

Figure 4. Diagnostic NOE connectivities (^{1}H NOESY) identifying the complexation of a series of aromatic acids inside the cavity for a representative sample of dimer and trimer complexes.

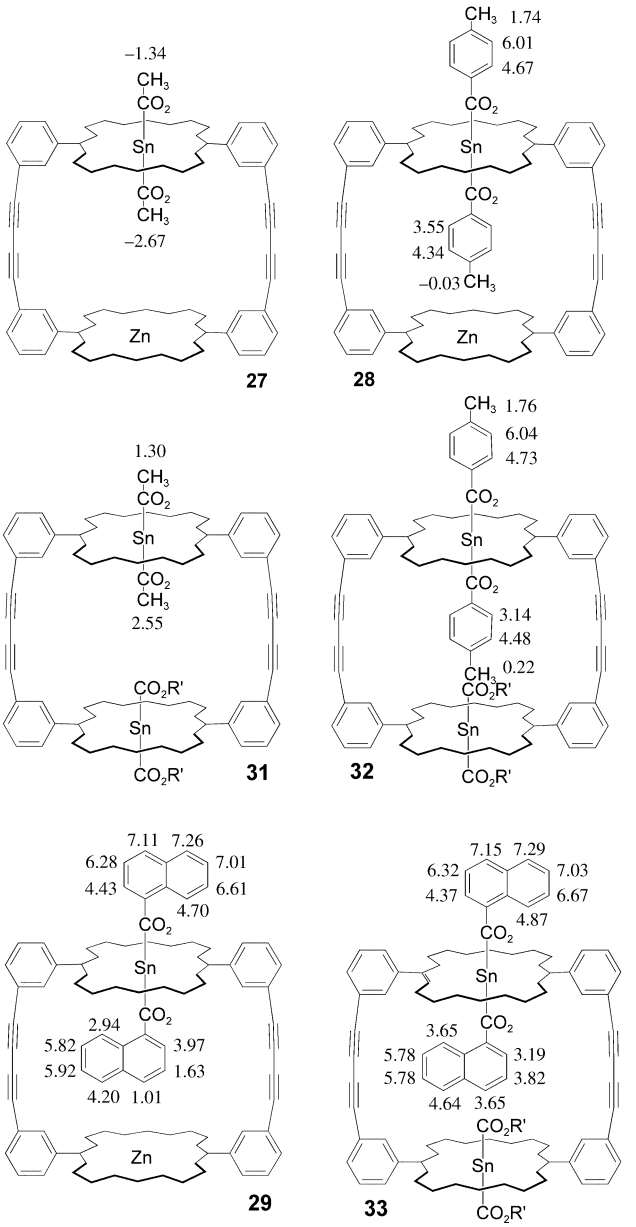

Figure 5. The proton NMR chemical shifts (ppm) are shown for acetic, *p*-toluic and 1-naphthoic acids bound to Sn_2- and SnZn dimers (**2** and **3**, respectively). The influence of the neighbouring-ring porphyrin ring currents on the intra- and extracavity ligands is reflected in the chemical shift of the protons of the two types of ligands. (The proton atoms have been omitted for clarity.)

on **5** was thus provided. For each of these examples no evidence was obtained to indicate that the ligands adopted a single preferred orientation.

Comparison of the intra- and extracavity ligand ($ligand_{in}$ and $ligand_{out}$, respectively) resonances in the ^{1}H NMR spectrum of carboxylate complexes of the SnZn dimer **3** and Sn_2 dimer **2** allowed assessment of the contribution of the second porphyrin to the shielding of the intracavity ligands (Figure 5). Likewise, the contribution of the porphyrin ring currents of Sn_3 trimer **4** on any $ligand_{in}$, which will inevitably include the corresponding contribution of the ring currents of the other bound neighbouring aromatic ligands, can be detected (for example **36**, Figure 6). The magnitude of the difference in the *trans* cavity ring current between cyclic porphyrin dimer **2** and trimer **4** was revealed by comparison of the $ligand_{in}$ proton chemical shifts of **31** and **35**, or **32** and **36**. The resonances of ligand protons and NOEs observed in the SnZn dimer complex of a given carboxylate differed from those of the corresponding Sn_2 dimer complex; compare for example **29** and **33**. Where $ligand_{in}$ ^{1}H NMR chemical-shift values differed by more than about 0.1 ppm between the $Sn(RCO_2)_2Zn$ and $Sn_2(RCO_2)_4$ dimer, the difference was considered to be too great to attribute to the magnitude of the ring current. Although the effect of a second intracavity ligand must be taken into account, the differences registered were interpreted to reflect primarily a difference in the geometry of the dimers.

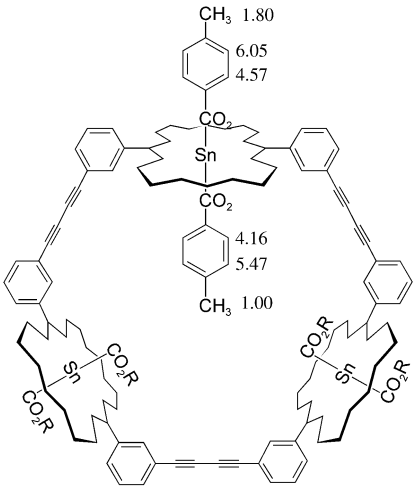

Figure 6. The proton NMR chemical shifts (ppm) are shown for *p*-toluic acid bound to the Sn_3-2,2,2-trimer **4**. As in the case of the 2,2-dimers, the influence of the neighbouring-ring porphyrin ring currents on the intra- and extracavity ligands is reflected in the chemical shift of the protons of the two types of ligands. (Only one pair of bound acids is shown, and the proton atoms have been omitted for clarity.)

process was taking place and allowed a geometry to be proposed for dimer **34**.

Corey–Pauling–Koltun space-filling models of the Sn_2(9-anthroate)$_4$ dimer implied that the Sn_2 dimer cavity could not accommodate two 9-anthroate ligands perpendicular to the Sn porphyrins, and that two intracavity groups could not rotate easily; the aromatic components of the inner ligands were constrained to be almost coplanar with the porphyrin (Scheme 2). The proximity of the large π-electron system of the 9-anthroate ligands to the host molecule was rationalised to influence the chemical shift of the porphyrin protons, and thereby impose a loss of symmetry on the porphyrin. Specifically, the peripheral porphyrin resonances became doubled due to loss of symmetry, according to their position with respect to the ligand, and all the methylene protons became nonequivalent.

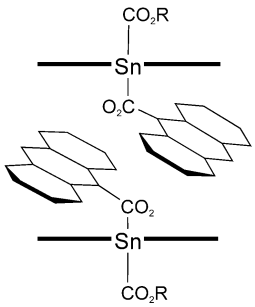

Scheme 2. Schematic side view of dimer **34**. (Steric demands are implied but not shown.)

Sn_2(9-anthroate)$_4$-2,2 dimer 34: Dimer **34** exhibited spectroscopic and structural characteristics unlike those of the Sn_2 dimer complexes of other carboxylates. The coordination of 9-anthroate groups resulted in the ^{1}H NMR spectrum of **34** being far more complicated than the analogous spectra of $Sn_2(RCO_2)_4$-2,2 dimers. Multiple porphyrin resonances in the ^{1}H NMR spectrum of dimer **34** were indicative of a loss of symmetry; two *meso*-proton resonances, four singlets attributable to pyrrole methyl and methoxy groups, and up to eight methylene-proton multiplets were observed. The COSY spectrum of **34** revealed this pattern of resonances to be due to the presence of two propionate chains, each with nonequivalent methylene protons giving a total of eight different methylene resonances. Single porphyrin aryl resonances and peaks corresponding to one inner and one outer ligand were also observed. The assignment of COSY and ROESY spectra indicated that the outer ligands rotated rapidly, such that the dimer experienced an averaged effect due to their presence. While the two intracavity coordinated ligands were chemically equivalent, the steric limitations imposed twofold symmetry on the host molecule, and as their rotation was slow on the NMR timescale, the peripheral porphyrin protons appeared to exchange between two environments (Figure 7). Identification of NOE and exchange cross peaks through the acquisition of a ROESY spectrum confirmed that an exchange

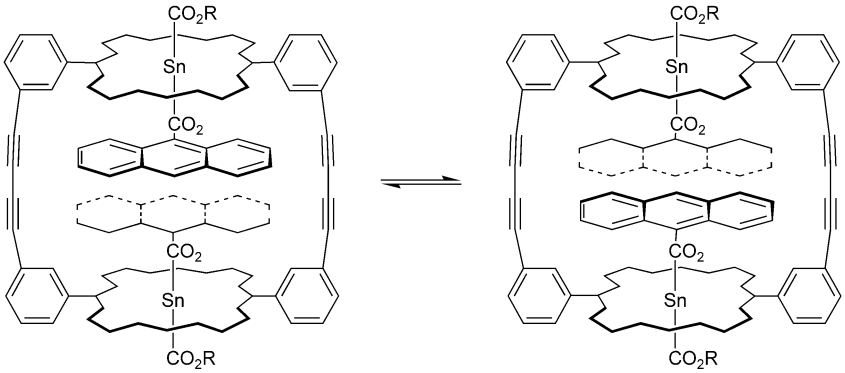

Figure 7. The Sn_2(9-anthroate)$_4$-2,2 dimer **34**. Slow rotation (on the NMR timescale) of the ligands discriminates between one ligand projecting forwards and one receding from the plane of the page. The symmetry established is reflected in the overall structure of **34** (see later).

NOE cross peaks between nonequivalent pyrrole methyl groups and one aromatic system were consistent with a ligand conformation in which the longest axis of each 9-anthroate group was aligned with the *meso* protons (Figure 8a). A geometry in which the ligands were aligned with the aryl groups, would also impose twofold symmetry on the dimer, but in this case just one *meso* proton resonance would be observed (with NOEs to nonequivalent methylene groups).

In the ROESY spectrum (298 K), each *meso* proton of **34** exhibited four NOEs to methylene groups substituted α to the porphyrin; this corresponded to the total number of **a**-type methylene protons. Exchange cross peaks were observed for all peripheral porphyrin protons; the two *meso*-proton resonances were identified by a connecting exchange peak, as were the two pyrrole methyl and the two methoxy groups (Figure 8a). Each methylene proton appeared to be in exchange with two other methylene protons.

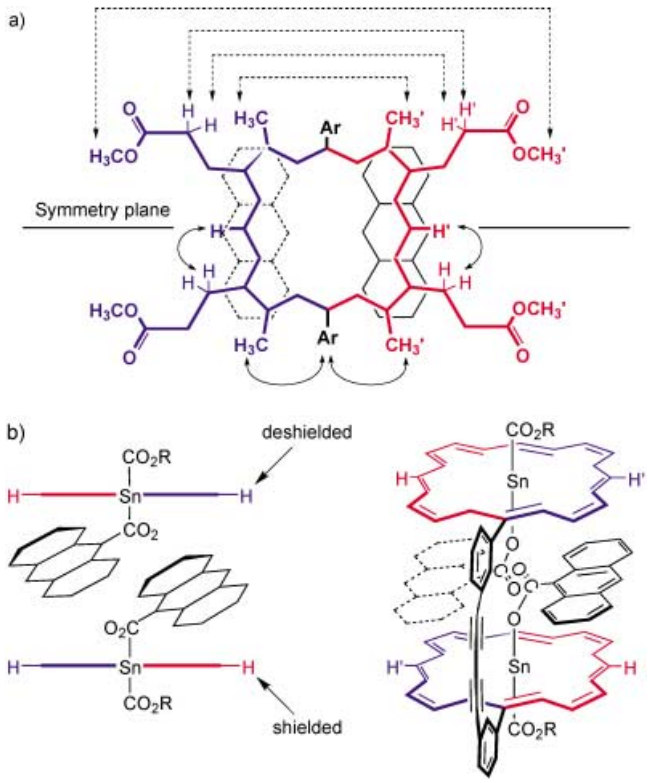

Figure 8. a) The symmetry that is established as a result of the two orientations of the cavity-bound ligands is shown, whereby sets of proton resonance in the ^{1}H NMR spectrum are attributed to the two halves of the porphyrins represented by the two different colours. In this representation, the complex (**34**) is viewed from above one of the porphyrin planes. The anthroate ligand closer to the porphyrin plane shown in this schematic is represented in solid lines, while the second cavity-bound aromatic ligand, which will sit further from the porphyrin plane, is represented in dotted lines. Solid arrows between specific protons establish NOE connectivities across the two halves of the molecules, while dotted arrows between specific protons identify sites which are exchanging on the NMR timescale. b) Side view of the complex described in a), showing the effect of the aromatic ligands on the porphyrin substituents.

The acquisition of a ROESY spectrum of **34** at 276 K revealed that the complex underwent exchange at this lower temperature. However, differences were detected in the intensities of the *meso*-methylene NOE cross peaks, reflecting a temperature dependence of the exchange mechanism. This allowed the peripheral porphyrin resonances to be fully assigned; the *meso* proton that resonated at lower field exhibited more intense NOE cross peaks to the lower-field methylene resonances, which in turn were determined to be in greater proximity to the pyrrole methyl group that resonated at lower field. For every pair of nonequivalent protons, for example, CH_3 and CH_3', the lower-field resonance was always attributed to the same "side" of the porphyrin, as defined by the mirror plane through the *meso* positions. One "side" of each porphyrin could therefore be described as deshielded (relative to the tetrahydroxo molecule **2**) and the other as shielded. At 276 K, exchange cross peaks were observed between single "shielded" and "deshielded" methylene resonances.

By considering the location of the inner ligands with respect to the dimer, the shielding/deshielding affect on the porphyrin resonances could be rationalised (Figure 8b). As viewed in the figure, one *meso* proton of the upper porphyrin is deshielded by edge-on exposure to the anthroate ligand coordinated to the lower porphyrin, while the same ligand shields the "facing" *meso* proton of the lower porphyrin. As the conformation of the ligands changed with rotation, the porphyrin protons experienced "shielded" and "deshielded" environments. The upper and lower porphyrins (or equally the shielded and deshielded protons) were related about a rotational axis of symmetry through the centre of the butadiyne links.

In view of the steric congestion within the Sn_2(9-anthroate)$_4$-2,2 dimer, the formation of **34** was unexpected; once one anthroate group is coordinated to an inner Sn porphyrin face, the angle at which a second ligand can enter must be limited. It may be that a weak interaction between the 9-anthroate ligand and porphyrin, of the type postulated to account for the coplanar conformation of the ligand and porphyrin in Sn(9-anthroate)$_2$TPP, promotes the formation of the Sn_2(9-anthroate)$_4$-2,2 dimer.[3]

Experimental Section

For column chromatography on alumina either neutral or basic Brockmann I (standard grade, 150 mesh) alumina was employed. Brockmann grades IV and V alumina were prepared by the addition of water (10 % and 15 % *w*/*w*, respectively), shaking and allowing the mixture to equilibrate for several hours. Chloroform employed in the preparation or reaction of $Sn(OH)_2$ porphyrins was passed through a short column of neutral alumina immediately prior to use. H_2TPP was used as obtained (Aldrich) without further purification.

Improved results for inserting tin(II) into porphyrins were obtained with anhydrous Sn dichloride ground into a fine powder in place of Sn dichloride dihydrate. By increasing the volume of pyridine or concentration of Sn salt, complete reaction was reliably achieved. The product was precipitated from the reaction mixture by addition of water and collected on celite. After extraction with chloroform, a hydrochloric acid wash was introduced to the work-up to ensure that all traces of Sn salts and pyridine were removed. Washing with water then completed the procedure.

^{1}H NMR spectra were recorded on Bruker DRX-400 or DRX-500 spectrometers (400 and 500 MHz, respectively). ^{13}C NMR spectra were obtained on an Bruker DRX-400 spectrometer operating at 100.6 MHz. All NMR measurements were carried out at room temperature in deuterochloroform unless otherwise specified. Two-dimensional NMR spectra were acquired by using standard Bruker pulse programs, with a relaxation delay of 2 s and 2048 data points in t_2. Typically, 16 scans were accumulated for 640 increments in t_1. Prior to FT, zero filling was applied to t_1 (1 K), and the data were multiplied by a shifted sine-bell function (qsine) in both domains.

Routine UV/visible spectra were obtained on a HP 8452 diode-array spectrophotometer in 10 mm oven-dried cuvettes. Distilled solvents were used throughout and, when used dry, were freshly obtained from solvent stills. Triethylamine and dichloromethane were distilled from CaH_2 under argon, while toluene and tetrahydrofuran were distilled from CaH_2 or sodium, also under argon. Free-base porphyrins were converted into zinc/nickel complexes in near quantitative yield by treatment with zinc/nickel acetate dihydrate in CH_2Cl_2 or heating at reflux with chloroform, respectively. MALDI-TOF mass spectra were recorded on a Kratos Analytical Ltd, Kompact MALDI IV mass spectrometer. A nitrogen laser (337 nm, 85 kW peak laser power, 3 ns pulse width) was used to desorb the sample ions, and the instrument was operated in linear time-of-flight mode with an accelerating potential of 20 kV. Results from 50 laser shots were signal-averaged to give one spectrum. An aliquot (1 μL) of a saturated

solution of the matrix (sinapinic acid) was deposited on the sample plate surface. Before the matrix completely dried, a small volume (1 μL) of analytes (dissolved in dichloromethane/chloroform at 1 mg mL^{-1}) was layered on the top of the matrix and allowed to air-dry.

Purification of diaion resin WA30: Ion-exchange resin WA30 (Supelco) was placed in a column (gravity packing). A volume of aqueous hydrochloric acid (2 M) equal to twice the volume of resin was passed through the column under gravity, water was then filtered through until the eluent was neutral. The procedure was repeated with aqueous sodium hydroxide (2.5 M) in place of aqueous hydrochloric acid, and the beads were then washed successively with methanol and chloroform, dried in vacuo and stored until required.

$SnCl_2$TPP 9: H_2TPP **8** (up to 500 mg) was stirred under reflux with finely ground anhydrous tin(II) chloride (2.4 equivalents) in pyridine (to give a porphyrin concentration of 0.01 M) for one hour. Complete Sn insertion was confirmed by UV spectroscopic examination of a drop of reaction mixture diluted with dichloromethane or chloroform. The crude product was precipitated by the addition of water (typically mL quantities) and collected by vacuum filtration on celite. Methanol (typically mL quantities) was washed through the celite plug to remove excess water, followed by chloroform to extract the porphyrin. The chloroform filtrate was washed with aqueous hydrochloric acid (6 M, typically 2×10 mL) and water ($3\times$ equal volume to organic solution), then dried (anhydrous sodium sulfate). Evaporation of the organic solution under reduced pressure gave a purple solid (90% yield prior to recrystallisation). ^{1}H NMR (250 MHz, $CDCl_3$) $\delta = 7.85$ (m, 12H; *m*- and *p*-aryl H), 8.34 (m, 8H; *o*-aryl H), 9.23 (s, Sn_{sat} ^4J(Sn-H) = 15.5 Hz, 8H; β-pyrrole H); ^{13}C NMR (62.5 MHz, $CDCl_3$) $\delta = 121.2$ (*meso*-C), 127.1 (C-3), 128.6 (C-4), 132.7 (C-β), 134.9 (C-2), 140.6 (C-1), 146.4 (C-α); UV/Vis (CH_2Cl_2) $\lambda_{max} = 404.3$, 425.7, 560.2, 599.8 nm.

$SnCl_2$ monomer 6: H_2 monomer **5** was heated under reflux with finely ground anhydrous tin(II) chloride (5 equivalents) in pyridine (porphyrin concentration of 0.005 M) for two hours and worked up as described for Sn insertion in to H_2TPP. Compound **6** was a red powder (typically 90% yield prior to recrystallisation). ^{1}H NMR (250 MHz, $CDCl_3$) $\delta = 0.27$ (s, 18H; $Si(CH_3)_3$), 2.66 (s, 12H; pyrrole CH_3), 3.30 (t, $^3J = 7.7$ Hz, 8H; $CH_2CH_2CO_2CH_3$), 3.66 (s, 12H; OCH_3), 4.23 (t, $^3J = 7.7$ Hz, 8H; $CH_2CH_2CO_2CH_3$), 7.80 (m, 2H; aryl H), 7.98 (m, 2H; aryl H), 8.00 (m, 2H; aryl H), 8.18 (m, 2H; aryl H), 10.84 (s, 2H; *meso*); ^{13}C NMR (62.5 MHz, $CDCl_3$) $\delta = -0.1$ ($Si(CH_3)_3$), 15.8 (pyrrole CH_3), 21.9 ($CH_2CH_2CO_2CH_3$), 36.3 ($CH_2CH_2CO_2CH_3$), 51.9 (OCH_3), 95.7 (aryl-C≡C), 97.5 (*meso*-CH), 104.3 (≡C–$Si(CH_3)_3$), 118.6 (*meso*-C), 123.5 (C-1), 128.1 (CH), 132.7 (CH), 132.9 (CH), 136.6 (CH), 140.6 (C_q), 141.1 (C_q), 142.6 (C_q), 142.7 (C_q), 143.7 (C_q), 173.3 (CO); UV/Vis (CH_2Cl_2) $\lambda_{max} =$ 396.8, 418.5, 547.7, 582.6 nm.

$Sn(OH)_2$porphyrins

Hydrolysis of $SnCl_2$ porphyrins: $SnCl_2$ porphyrin (100 mg scale) was dissolved in the minimum volume of dichloromethane or chloroform and stirred with basic alumina (activity V, 1.6 g per 0.1 mmol of porphyrin) for five hours. The resulting slurry was filtered, the filtrate was dried (sodium sulfate), the solvent was removed under reduced pressure, and the residue was recrystallised by layered addition of hexane to a concentrated solution in dichloromethane. Purple (**10**) or red (**7**) powder was obtained (typical yield 80% from free-base porphyrin).

*Sn(OH)$_2$TPP **10***: ^{1}H NMR (250 MHz, $CDCl_3$) $\delta = -7.44$ (br s, 2H; OH), 7.81 (m, 12H; *m* -and *p*-aryl H), 8.34 (m, 8H; *o*-aryl H), 9.13 (s, Sn_{sat} ^4J(Sn-H) = 10.1 Hz, 8H; β-pyrrole H); ^{13}C NMR (62.5 MHz, $CDCl_3$) $\delta = 121.4$ (*meso*-C), 127.1 (C-3), 128.4 (C-4), 132.8 (C-β), 135.2 (C-2), 141.4 (C-1), 146.9 (C-α); UV/Vis (CH_2Cl_2) $\lambda_{max} = 402.8$, 424.0, 558.6, 598.3 nm.

$Sn(OH)_2$ monomer 7: ^{1}H NMR (250 MHz, $CDCl_3$) $\delta = -7.81$ (br s, 2H; OH), 0.27 (s, 18H; $Si(CH_3)_3$), 2.61 (s, 12H; pyrrole CH_3), 3.31 (t, 8H; $^3J =$ 7.7 Hz, $CH_2CH_2CO_2CH_3$), 3.74 (s, 12H; OCH_3), 4.44 (t, $^3J = 7.7$ Hz, 8H; $CH_2CH_2CO_2CH_3$), 7.77 (m, 2H; aryl H), 7.98 (m, 2H; aryl H), 8.14 (m, 2H; aryl H), 8.25 (m, 2H; aryl H), 10.71 (s, 2H; *meso*); ^{13}C NMR (62.5 MHz, $CDCl_3$) $\delta = -0.1$ ($Si(CH_3)_3$), 15.6 (CH_3), 21.8 ($CH_2CH_2CO_2CH_3$), 36.5 ($CH_2CH_2CO_2CH_3$), 51.9 (OCH_3), 95.4 (aryl-C≡C), 97.8 (*meso*-CH), 104.5 (≡C–$Si(CH_3)_3$), 118.8 (*meso*-C), 123.3 (C-1), 128.1 (CH), 132.6 (CH), 133.0 (CH), 136.4 (CH), 140.4 (C_q), 141.9 (C_q), 142.5 (C_q), 142.9 (C_q), 144.1 (C_q), 173.4 (CO); UV/Vis (CH_2Cl_2) $\lambda_{max} = 398.7$, 416.9, 546.8, 581.8 nm.

$Sn(RCO_2)_2$ porphyrins

Preparative-scale synthesis of $Sn(RCO_2)_2$ porphyrins: A carboxylic acid (2.4 equivalents) was added to $Sn(OH)_2$ porphyrin (10 mg scale) in chloroform. The solution was stirred for 30 minutes, sodium sulfate was then added, and the mixture was stirred for a further 2–3 minutes. After filtration and removal of the solvent (reduced pressure), the pure complex was isolated by recrystallisation from dichloromethane and hexane (~70% recovery).

Complete formation of the dicarboxylate complex was always observed, for this reason the binding of the carboxylate was not followed spectroscopically but assumed to go to completion.

*Sn(propionate)$_2$TPP **11***: ^{1}H NMR (250 MHz, $CDCl_3$) $\delta = -1.42$ (t, $^3J =$ 7.6 Hz, 6H; CH_3), −0.78 (q, $^3J = 7.6$ Hz, 4H; CH_2), 7.80 (m, 12H; *m*- and *p*-aryl H), 8.30 (m, 8H; *o*-aryl H), 9.17 (s, Sn_{sat} ^4J (Sn–H) = 14.5 Hz, 8H; β-pyrrole H); ^{13}C NMR (62.5 MHz, $CDCl_3$) $\delta = 8.1$ (CH_3), 27.6 (CH_2), 121.5 (*meso*-C), 126.9 (C-3), 128.3 (C-4), 132.5 (C-β), 134.7 (C-2), 141.1 (C-1), 147.1 (C-α), 171.3 (CO); UV/Vis (CH_2Cl_2) $\lambda_{max} = 401.4$, 422.6, 556.5, 595.3 nm.

*Sn(acetate)$_2$TPP **12***: ^{1}H NMR (250 MHz, $CDCl_3$) $\delta = -1.05$ (s, 6H; CH_3), 7.82 (m, 12H; *m*- and *p*-aryl H), 8.29 (m, 8H; *o*-aryl H), 9.18 (s, Sn_{sat} ^4J (Sn-H) = 14.6 Hz, 8H; β-pyrrole H); ^{13}C NMR (62.5 MHz, $CDCl_3$) $\delta = 20.7$ (CH_3), 121.5 (*meso*-C), 126.9 (C-3), 128.4 (C-4), 132.5 (C-β), 135.1 (C-2), 141.0 (C-1), 147.0 (C-α), 168.4 (CO); UV/Vis (CH_2Cl_2) $\lambda_{max} = 401.3$, 422.5, 556.6, 595.7 nm.

*Sn(chloroacetate)$_2$TPP **13***: ^{1}H NMR (250 MHz, $CDCl_3$) $\delta = 0.93$ (s, 4H; CH_2Cl), 7.82 (m, 12H; *m*- and *p*-aryl H), 8.31 (m, 8H; *o*-aryl H), 9.21 (s, ^4J (Sn-H) = 15.5 Hz, 8H; β-pyrrole H); ^{13}C NMR (62.5 MHz, $CDCl_3$) $\delta = 40.6$ (CH_2Cl), 121.8 (*meso*-C), 127.0 (C-3), 128.5 (C-4), 132.8 (C-β), 134.8 (C-2), 140.7 (C-1), 147.2 (C-α), 162.9 (CO); UV/Vis (CH_2Cl_2) $\lambda_{max} = 400.4$, 421.3, 554.3, 594.1 nm.

*Sn(dichloroacetate)$_2$TPP **14***: ^{1}H NMR (250 MHz, $CDCl_3$) $\delta = 2.85$ (s, 2H; $CHCl_2$), 7.82 (m, 12H; *m*- and *p*-aryl H), 8.31 (m, 8H; *o*-aryl H), 9.24 (s, Sn_{sat} ^4J (Sn-H) = 16.1 Hz, 8H; β-pyrrole H); ^{13}C NMR (62.5 MHz, $CDCl_3$) $\delta = 64.8$ ($CHCl_2$), 121.8 (*meso*-C), 127.0 (C-3), 128.6 (C-4), 132.9 (C-β), 134.7 (C-2), 140.6 (C-1), 147.3 (C-α), 159.4 (CO); UV/Vis (CH_2Cl_2) $\lambda_{max} =$ 399.0, 420.1, 553.9, 592.2 nm.

Small (^{1}H NMR) scale preparation of $Sn(RCO_2)_2$ porphyrin complexes from carboxylic acid solutions: $Sn(OH)_2$ porphyrin (ca. $2.5-3.0 \times 10^{-3}$ mmol) was carefully transferred to an NMR tube with dried (alumina filtered) [D]chloroform (0.5 mL). A solution of the carboxylic acid in the same solvent (0.26 M, volume of 0.5 mL) was prepared. Two equivalents of the carboxylic acid solution (20 μL) were injected into the porphyrin solution and the sample was shaken well.

For carboxylic acids that were not soluble in neat [D]chloroform at a concentration of approx. 0.25 M, a solution of the acid in [D_4]methanol/[D]chloroform (3:2) was prepared. No other changes to the technique were required.

Small (^{1}H NMR) scale preparation of $Sn(RCO_2)_2$ porphyrin complexes from solid carboxylic acids: $Sn(OH)_2$ porphyrin (typically $2.5-3.0 \times 10^{-3}$ mmol) and carboxylic acid (2 equivalents) were combined with a volume of dried [D]chloroform (alumina filtered; 0.6 mL) in a 2 mL vial and stirred for three hours. The solution was then transferred to an NMR tube.

Cyclic Sn porphyrin oligomers

*Sn_2Cl_4 dimer **1***: H_4 dimer (50 mg, 0.0275 mmol) was heated at reflux with finely ground anhydrous tin(II) chloride (52 mg, 0.275 mmol) in pyridine (70 mL) for two hours. The disappearance of low-wavelength Q-bands in the UV spectrum indicated complete metallation. After being cooled to room temperature, the volume of the reaction mixture was reduced to ~10 mL by distillation under reduced pressure. The residual concentrated pyridine solution was then diluted with chloroform and cautiously washed with aqueous hydrochloric acid (6 M, 3×200 mL) and water (3×400 mL). Evaporation of the chlorinated solvent under reduced pressure afforded the product as a red solid (57 mg, 94% not recrystallised). ^{1}H NMR (250 MHz, $CDCl_3$) $\delta = 2.45$ (s, 24H; pyrrole CH_3), 3.07 (t, $^3J = 7.5$ Hz, 16H; $CH_2CH_2CO_2CH_3$), 3.56 (s, 24H; OCH_3), 4.26 (m, 16H; $CH_2CH_2CO_2CH_3$), 7.35 (s, 4H; *o*-$aryl_{in}$ H), 7.80 (m, 8H; aryl H), 8.48 (m, 4H; *o*-$aryl_{out}$ H), 10.49 (s, 4H; *meso*); ^{13}C NMR (62.5 MHz, $CDCl_3$) $\delta = 15.6$ (pyrrole CH_3), 21.6 ($CH_2CH_2CO_2CH_3$), 36.2 ($CH_2CH_2CO_2CH_3$), 51.7 (OCH_3), 75.7 (C≡C), 83.7

(C≡), 97.3 (*meso*-CH), 117.8 (*meso*-C), 122.0 (C-1), 127.7 (CH), 128.8 (CH), 132.5 (CH), 140.1 (C_q), 140.3 (CH), 141.3 (C_q), 142.2 (C_q), 142.4 (C_q), 143.3 (C_q), 173.2 (CO); UV/Vis (CH_2Cl_2) $\lambda_{max} = 416.6$, 549.1, 584.3 nm.

$Sn_2(OH)_4$ dimer ***2***: Without further purification, dimer **1** (57 mg, 0.026 mmol) was stirred with activated diaion WA30 resin (3.47 g, 5.2 mmol) and water (9.4 μL, 0.52 mmol) in chloroform (250 mL) for 6 h. The resin was filtered from the reaction mixture, and the chloroform solution was washed with water (2 × 200 mL) and dried (sodium sulfate). The organic solvent was removed, and the residue was recrystallised from dichloromethane and hexane to yield a fine red powder (29 mg, 50% overall yield from the H_4 dimer). ^{1}H NMR (250 MHz, $CDCl_3$) $\delta = -9.02$ (br s, 2H; OH_{in}), −7.86 (br s, 2H; OH_{out}), 2.41 (s, 24H; pyrrole CH_3), 3.06 (t, 16H; $^3J = 7.5$ Hz, $CH_2CH_2CO_2CH_3$), 3.65 (s, 24H; OCH_3), 4.23 (t, 16H; $^3J = 7.5$ Hz, 16H; $CH_2CH_2CO_2CH_3$), 7.57 (s, 4H; *o*-$aryl_{in}$ H), 7.77 (m, 8H; aryl H), 8.36 (m, 4H; *o*-$aryl_{out}$ H), 10.36 (s, 4H; *meso*); ^{13}C NMR (62.5 MHz, $CDCl_3$) $\delta = 15.5$ (pyrrole CH_3), 21.6 ($CH_2CH_2CO_2CH_3$), 36.4 ($CH_2CH_2CO_2CH_3$), 51.8 (OCH_3), 75.9 (C≡C), 84.4 (C≡C), 97.3 (*meso*-CH), 118.0 (*meso*-C), 121.9 (C-1), 127.7 (CH), 129.7 (CH), 132.4 (CH), 140.7 (CH), 139.9 (C_q), 142.0 (C_q), 142.2 (C_q), 142.5 (C_q), 143.8 (C_q), 173.3 (CO); UV/Vis (CH_2Cl_2) $\lambda_{max} = 415.0$, 547.9, 583.4 nm.

$Sn_3(OH)_6$ trimer ***4***: The Sn_3Cl_6 trimer was prepared, in the same way as the Sn_2Cl_4 dimer, from the H_6 trimer (35 mg, 0.013 mmol), anhydrous tin(II) chloride (36.9 mg, 0.195 mmol) and pyridine (40 mL). Repeated attempts were made to extract the pyridine reaction mixture with chloroform, but much of the porphyrin material remained in the suspension. However, the combined chloroform fractions were stirred with diaion WA30 resin (2.6 g, 3.9 mmol) and water (7 μL, 0.39 mmol) without further purification or characterisation to yield the $Sn_3(OH)_6$-2,2,2 trimer, which was recrystallised from dichloromethane and hexane (18 mg, 28%). ^{1}H NMR (250 MHz, $CDCl_3$) $\delta = 2.52$ (s, 36H; pyrrole CH_3), 3.17 (t, $^3J = 7.5$ Hz, 24H; $CH_2CH_2CO_2CH_3$), 3.63 (s, 36H; OCH_3), 4.33 (t, $^3J = 7.5$ Hz, 24H; $CH_2CH_2CO_2CH_3$), 7.80 (dd, $^3J = 7.5$ Hz, 6H; *m*-aryl H), 8.07 (d, $^3J = 7.5$ Hz, 6H; aryl H), 8.16 (d, $^3J = 7.5$ Hz, 6H; aryl H), 8.22 (s, 6H; *o*-$aryl_{in}$ H), 10.60 (s, 6H; *meso*); ^{13}C NMR (62.5 MHz, $CDCl_3$) $\delta = 15.5$ (pyrrole CH_3), 21.7 ($CH_2CH_2CO_2CH_3$), 36.3 ($CH_2CH_2CO_2CH_3$), 51.8 (OCH_3), 74.8 (C≡C), 81.4 (C≡C), 97.8 (*meso*-CH), 118.2 (*meso*-C), 121.8 (C-1), 128.3, 128.9, 132.4, 133.0, 140.1, 142.2, 142.5, 142.8, 143.9, 173.3 (CO); UV/Vis (CH_2Cl_2) $\lambda_{max} =$ 416.1, 547.4, 581.7 nm.

Asymmetric cyclic porphyrin dimers

$Sn(OH)_2$Zn dimer ***3***: Zinc acetate dihydrate (29 mg, 0.132 mmol) was dissolved in the minimum volume of methanol, diluted with chloroform (1 mL), and this mixture was added dropwise to a rapidly stirred solution of the H_4 dimer **20** (300 mg, 0.165 mmol) in chloroform (200 mL). The mixture was stirred for a further 20 minutes; tlc (alumina; chloroform) confirmed the presence of three differentially metallated products. The solvent was removed (reduced pressure), and the crude dimer mixture was dried in vacuo to remove all traces of methanol.

Column chromatography (7 cm, neutral activity IV alumina) eluting with chloroform/dichloromethane (1:4) under gravity yielded the H_4 dimer (113 mg). The eluent was changed to chloroform/dichloromethane (1:2.3) to ensure that all the H_4 dimer **20** was eluted before the column was flushed with chloroform to collect both the H_2Zn dimer **21** and Zn_2 dimer **22**. The solvent was removed (affording 178 mg of mixed dimers), and the residue was treated with anhydrous tin(II) chloride (88.4 mg, 0.47 mmol) in pyridine (15 mL), as described for the preparation of the Sn_2Cl_4 dimer **1**. Washing the pyridine/chloroform solution of the product with aqueous hydrochloric acid (6M, 3 × 200 mL) gave the $SnCl_2H_2$ dimer **24** and H_4 dimer **20**. After three aqueous washes, the organic phase was dried (sodium sulfate) and the solvent was evaporated under reduced pressure to afford 169 mg of mixed dimers.

Dimer **20** was separated from the Sn free-base dimer fraction by additional column chromatography (7 cm, neutral activity IV alumina; chloroform/dichloromethane, 1:2.3), 41.5 mg were obtained. Subsequent elution with chloroform yielded 84.6 mg of $SnCl_X(OH)_YH_2$-2,2-dimer after removing the solvent under reduced pressure. The dimer was redissolved in chloroform (100 mL), and zinc chloride (15 mg, 0.11 mmol) was added to the solution. A few drops each of methanol and triethylamine were added to aid solubility of the Zn salt and prevent protonation of the free-base porphyrin by hydrochloric acid. The mixture was stirred at room temperature until UV analysis showed metallation to be complete (~20 minutes). Two aqueous washes of the resulting $SnCl_X(OH)_Y$Zn-2,2-dimer solution were then carried out, the organic phase was subsequently dried over sodium sulfate and evaporated to afford 87.9 mg.

Water (1 μL, 0.5 mmol) and diaion resin WA30 (0.73 g, 1.1 mmol) were added to a solution of the dimer dissolved in chloroform (50 mL), and the mixture was stirred for 2 h. $Sn(OH)_2$Zn dimer **3** was separated from the resin by filtration as previously (see synthesis of dimer **2**). Removal of the solvent left a red residue, which was recrystallised from dichloromethane and hexane to give 53.4 mg of a red powder. Overall yield from H_4 dimer **20** of 16%; 51% (without recrystallisation) of the porphyrinic starting material was recovered as the H_4 dimer. ^{1}H NMR (250 MHz, $CDCl_3$) $\delta = -8.72$ (br s, 2H; OH_{in}), −7.56 (br s, 2H; OH_{out}), 2.29 (s, 12H; Zn-pyrrole CH_3), 2.44 (s, 12H; Sn-pyrrole CH_3), 2.93 (t, $^3J = 7.5$ Hz, 8H; Zn-$CH_2CH_2CO_2CH_3$), 3.09 (t, $^3J = 7.5$ Hz, 8H; Sn-$CH_2CH_2CO_2CH_3$), 3.61 (s, 12H; Zn-OCH_3), 3.62 (s, 12H; Sn-OCH_3), 4.08 (t, $^3J = 7.5$ Hz, 8H; Zn-$CH_2CH_2CO_2CH_3$), 4.25 (t, $^3J = 7.5$ Hz, 8H; Sn-$CH_2CH_2CO_2CH_3$), 7.17 (s, 2H; Zn-*o*-$aryl_{in}$ H), 7.36 (s, 2H; Sn-*o*-$aryl_{in}$ H), 7.73 (m, 4H; Zn-aryl H), 7.80 (m, 4H; Sn-aryl H), 8.43 (m, 2H; Zn-*o*-$aryl_{out}$ H), 8.51 (m, 2H; Sn-*o*-$aryl_{out}$ H), 9.80 (s, 2H; Zn-*meso*), 10.42 (s, 2H; Sn-*meso*); ^{13}C NMR (62.5 MHz, $CDCl_3$) $\delta = 15.6$ (Sn and Zn-pyrrole CH_3), 21.6 (Sn and Zn-$CH_2CH_2CO_2CH_3$), 36.3 ($CH_2CH_2CO_2CH_3$), 36.8 ($CH_2CH_2CO_2CH_3$), 51.6 (OCH_3), 51.7 (OCH_3), 74.7 (C + C), 75.7 (C≡C), 83.1 (C≡C), 84.1 (C + C), 96.9 (*meso*-CH), 97.5 (*meso*-CH), 117.5 (*meso*-C), 118.1 (*meso*-C), 121.1 (C-1), 122.1 (C-1), 127.1, 127.6, 128.8, 129.5, 130.0, 130.9, 132.3, 133.0, 137.0 (C_q), 140.2 (C_q), 140.7 (C_q), 141.4 (C_q), 141.9 (C_q), 142.0 (C_q), 142.5 (C_q), 142.6 (C_q), 144.0 (C_q), 144.8 (C_q), 173.2 (CO), 173.4 (CO); UV/Vis (CH_2Cl_2) $\lambda_{max} = 413.6$, 507.2, 545.9, 580.4 nm.

H_2Zn dimer ***21***: Pure dimer **21** was collected in the chromatographic separation of H_4 dimer **20** from H_2Zn dimer **21** and Zn_2 dimer **22** (see synthesis of dimer **3**). ^{1}H NMR $\delta =$ (250 MHz, $CDCl_3$) −2.61 (br s, 2H; NH), 2.32 (s, 12H; Zn-pyrrole CH_3), 2.35 (s, 12H; H_2-pyrrole CH_3), 2.96 (m, 16H; H_2 and Zn-$CH_2CH_2CO_2CH_3$), 3.55 (s, 12H; OCH_3), 3.60 (s, 12H; OCH_3), 4.11 (m, 16H; H_2 and Zn-$CH_2CH_2CO_2CH_3$), 7.00 (s, 2H; Zn-*o*-$aryl_{in}$ H), 7.10 (s, 2H; H_2-*o*-$aryl_{in}$ H), 7.77 (m, 8H; H_2 and Zn-aryl H), 8.51 (m, 4H; H_2 and Zn-*o*-$aryl_{out}$ H), 9.90 (s, 2H; Zn-*meso*), 10.00 (s, 2H; H_2-*meso*); ^{13}C NMR $\delta =$ (62.5 MHz, $CDCl_3$) 14.9 (pyrrole CH_3), 15.7 (pyrrole CH_3), 21.7 (H_2 and Zn-$CH_2CH_2CO_2CH_3$), 36.7 ($CH_2CH_2CO_2CH_3$), 36.8 ($CH_2CH_2CO_2CH_3$), 51.6 (H_2 and Zn-OCH_3), 74.6 (C + C), 74.8 (C≡C), 82.7 (C≡C), 83.1 (C + C), 96.6 (*meso*-CH), 97.2 (*meso*-CH), 116.5 (*meso*-C), 117.7 (*meso*-C), 121.1 (C-1), 121.5 (C-1), 127.1, 127.4, 130.0, 130.3, 132.2, 132.9, 137.1, 139.1, 139.3, 140.7, 141.5, 141.5, 141.8, 143.2, 144.8, 145.5, 147.2, 173.3 (CO), 173.4 (CO);* FAB MS: *m/z*: 1881 [M^++H], calcd for $C_{112}H_{102}N_8O_{16}Zn$: 1881.5; UV/Vis ($CH_2Cl_2$) $\lambda_{max} = 410.8$, 507.8, 542.6, 576.4 nm. *One aromatic/pyrrole ^{13}C NMR resonance not resolved.

$SnCl_2$Zn dimer ***23***: A mixture of dimer **23** and Zn_2 dimer **22** was obtained as an intermediate in the synthesis of $Sn(OH)_2$Zn dimer **3**. Pure dimer **23** was prepared by methods employed for the synthesis of **3**. The H_2Zn dimer was heated under reflux with anhydrous tin(II) chloride and subsequently washed with aqueous hydrochloric acid to give the $SnCl_2H_2$ dimer. Treatment with zinc chloride yielded the $SnCl_2$Zn dimer. ^{1}H NMR (250 MHz, $CDCl_3$) $\delta = 2.26$ (s, 12H; Zn-pyrrole CH_3), 2.47 (s, 12H; Sn-pyrrole CH_3), 2.89 (t, $^3J = 7.5$ Hz, 8H; Zn-$CH_2CH_2CO_2CH_3$), 3.07 (t, $^3J =$ 7.5 Hz, 8H; Sn-$CH_2CH_2CO_2CH_3$), 3.48 (s, 12H; Zn-OCH_3), 3.61 (s, 12H; Sn-OCH_3), 4.03 (t, $^3J = 7.5$ Hz, 8H; Zn-$CH_2CH_2CO_2CH_3$), 4.27 (t, $^3J =$ 7.5 Hz, 8H; Sn-$CH_2CH_2CO_2CH_3$), 7.20 (s, 2H; Zn-*o*-$aryl_{in}$ H), 7.38 (s, 2H; Sn-*o*-$aryl_{in}$ H), 7.72 (m, 4H; Zn-aryl H), 7.81 (m, 4H; Sn-aryl H), 8.39 (m, 2H; Zn-*o*-$aryl_{out}$ H), 8.52 (m, 2H; Sn-*o*-$aryl_{out}$ H), 9.72 (s, 2H; Zn-*meso*), 10.50 (s, 2H; Sn-*meso*); ^{13}C NMR (100 MHz, $CDCl_3$) $\delta = 15.5$ (pyrrole CH_3), 15.6 (pyrrole CH_3), 21.6 (Sn and Zn-$CH_2CH_2CO_2CH_3$), 36.1 ($CH_2CH_2CO_2CH_3$), 36.8 ($CH_2CH_2CO_2CH_3$), 51.6 (OCH_3), 51.7 (OCH_3), 74.7 (C + C), 75.6 (C≡C), 83.1 (C≡C), 84.5 (C + C), 96.9 (*meso*-CH), 97.4 (*meso*-CH), 117.6 (*meso*-C), 117.9 (*meso*-C), 121.0 (C-1), 122.2 (C-1), 127.2, 127.7, 128.8, 129.3, 130.2, 130.9, 132.3, 132.9, 137.0, 138.5, 140.3, 141.1, 141.2, 142.2, 142.5, 143.3, 145.4, 147.1, 173.1 (CO), 173.4 (CO); UV/Vis (CH_2Cl_2) $\lambda_{max} = 415.3$, 545.2, 580.7 nm.

Small (^{1}H NMR) scale preparation of $Sn(RCO_2)_2$ porphyrin oligomers: $Sn(RCO_2)_2$ porphyrin oligomers were prepared in the same way as carboxylate complexes of Sn porphyrin monomers, with $Sn(OH)_2$ porphyrin oligomer (concentration 1.9 mM, [D]chloroform) and solutions of carboxylic acids in [D]chloroform or [D]chloroform/[D_4]methanol. Diag-

Table 1. ^{1}H NMR resonances for the $Sn(RCO_2)_2Zn$-2,2-dimer complexes.

Proton	**27**	**28**	**29**	**30**
Sn pyrrole CH_3	2.45	2.42	2.44	2.35
Sn $CH_2CH_2CO_2CH_3$	3.06	3.02	2.99	2.93
Sn OCH_3	3.59	3.57	3.46	3.34
Sn $CH_2CH_2CO_2CH_3$	4.28	4.27	4.24	4.15
Sn *o*-aryl$_{in}$	7.18	6.98	7.46	7.33
Sn *m*- and *p*-aryl	7.80	7.77	7.78	7.89
Sn *o*-aryl$_{out}$	8.63	8.55	8.29	8.51
Sn *meso*	10.46	10.49	10.50	10.34
Zn pyrrole CH_3	2.29	2.30	2.32	2.34
Zn $CH_2CH_2CO_2CH_3$	2.94	2.94	2.88	2.81
Zn OCH_3	3.48	3.46	3.34	3.30
Zn $CH_2CH_2CO_2CH_3$	4.10	4.11	4.09	4.06
Zn *o*-aryl$_{in}$	7.09	7.08	7.28	7.32
Zn *m*- and *p*-aryl	7.72	7.73	7.75	7.81
Zn *o*-aryl$_{out}$	8.47	8.47	8.41	8.47
Zn *meso*	9.85	9.87	9.91	9.89

Table 2. ^{1}H NMR resonances for the $Sn_2(RCO_2)_4$-2,2-dimer complexes.

Proton	**31**	**32**	**33**
pyrrole CH_3	2.47	2.45	2.45
$CH_2CH_2CO_2CH_3$	3.07	3.01	2.95
OCH_3	3.54	3.45	3.30
$CH_2CH_2CO_2CH_3$	4.28	4.28	4.23
o-aryl$_{in}$	7.06	6.88	7.15
m- and *p*-aryl	7.80	7.80	7.80
o-aryl$_{out}$	8.69	8.69	8.51
meso	10.42	10.49	10.52

Table 3. ^{1}H NMR resonances for the Sn_2(9-anthroate)$_4$-2,2 dimer **34**.

Proton	Shielded "side"	Deshielded "side"
pyrrole CH_3	2.23	2.66
$CH_2CH_2CO_2CH_3$	2.20 and 2.31	3.11 and 3.23
OCH_3	2.40	3.59
$CH_2CH_2CO_2CH_3$	3.51 and 4.11	4.35 and 4.46
o-aryl$_{in}$	7.56	7.56
m- and *p*-aryl	8.00	8.00
o-aryl$_{out}$	8.70	8.70
meso	10.35	10.78

Table 4. ^{1}H NMR resonances for the $Sn_3(RCO_2)_6$-2,2,2-trimer complexes.

Proton	**35**	**36**
pyrrole CH_3	2.55	2.49
$CH_2CH_2CO_2CH_3$	3.14	3.08
OCH_3	3.47	3.49
$CH_2CH_2CO_2CH_3$	4.37	4.37
o-aryl$_{in}$	8.17	7.91
m-aryl	7.79	7.75
p-aryl	8.06 or 8.18	8.03
o-aryl$_{out}$	8.06 or 8.18	8.03
meso	10.59	10.64

nostic ^{1}H NMR resonances for the cyclic oligomers **27**–**36** are shown in Tables 1–4 (500 MHz, $CDCl_3$, 298 K).

Acknowledgement

We thank the EPSRC, Unilever Research and the Morrell Fund for generous financial support, and Professor C. A. Hunter for useful discussions.

[1] J. K. M. Sanders, *Pure Appl. Chem.* **1996**, *72*, 2265.
[2] Z. Clyde-Watson, A. Vidal-Ferran, L. J. Twyman, C. J. Walter, D. W. J. McCallien, S. Fanni, N. Bampos, R. S. Wylie, J. K. M. Sanders, *New J. Chem.* **1998**, *22*, 493.
[3] J. C. Hawley, N. Bampos, R. J. Abraham, J. K. M. Sanders, *Chem. Commun*. **1998**, 661.
[4] H. L. Anderson, J. K. M. Sanders, *J. Chem. Soc. Perkin Trans. 1* **1995**, 2223; S. Anderson, H. L. Anderson, J. K. M. Sanders, *J. Chem. Soc. Perkin Trans. 1* **1995**, 2247.
[5] J. C. Hawley, N. Bampos, J. K. M Sanders, unpublished results.
[6] a) J. K. M. Sanders, *The Porphyrin Handbook*, *Vol. 3* (Ed.: K. M. Kadish, K. M. Smith, R. Guilard) Academic Press, San Diego, **2000**, p. 347; b) N. Bampos, Z. Clyde-Watson, J. C. Hawley, C. C. Mak, A. Vidal-Ferran, S. J. Webb, J. K. M. Sanders, *NMR in Supramolecular Chemistry* (Ed.: M. Pons), Kluwer, Dordrecht, **1999**, p. 37.
[7] a) J. E. Redman, N. Feeder, S. J. Teat, J. K. M. Sanders, *Inorg. Chem.* **2001**, *40*, 2486; b) B. G. Maiya, N. Bampos, A. A. Kumar, N. Feeder, J. K. M. Sanders, *New J. Chem.* **2001**, *25*, 797; c) S. J. Webb, J. K. M. Sanders, *Inorg. Chem.* **2000**, *39*, 5920; d) H. J. Kim, N. Bampos, J. K. M. Sanders, *J. Am. Chem. Soc.* **1999**, *121*, 8120.
[8] J. W. Buchler in *The Porphyrins*, *Vol. 1*, (Ed.: D. Dolphin), Academic Press, New York, **1978**, p. 36.
[9] D. P. Arnold, *J. Chem. Educ.* **1988**, *65*, 1111.
[10] M. J. Crossley, P. Thordarson, R. A.-S. Wu, *J. Chem. Soc. Perkin 1* **2001**, 2294.
[11] As Sn porphyrins bind irreversibly to silica, their reactions cannot generally be followed by silica tlc. For Sn insertion, silica tlc can be used to determine whether free-base porphyrin is present.
[12] D. P. Arnold, *Polyhedron* **1986**, *5*, 1957.
[13] D. P. Arnold, E. A. Morrison, J. V. Hanna, *Polyhedron* **1990**, *9*, 1331.
[14] S. J. Langford, M. A. P. Lee, K. J. Macfarlane, J. A. Weigold, *J. Inclusion Phenom. Macrocyclic Chem.* **2001**, *41*, 135.
[15] Stirring $SnCl_2$ porphyrin with a carboxylic acid under parallel conditions did not result in the formation of a tin porphyrin carboxylate complex.
[16] R. J. Abraham, C. J. Medforth, *Magn. Reson. Chem.* **1987**, *25*, 432; R. J. Abraham, I. Marsden, *Tetrahedron* **1992**, *48*, 7489.
[17] G. Smith, D. P. Arnold, C. H. L. Kennard, T. C. W. Mak, *Polyhedron* **1991**, *10*, 509.
[18] E. Heller, G. M. J. Schmidt, *Isr. J. Chem.* **1971**, *9*, 449.

Received: February 19, 2003 [F4862]